

Fine-grained mommagraphy object detection with multiple feature fusion transfer learning

Ri-Gui Zhou^{a,b}, Shihao Lv^{a,b,*}, Yaochong Li^{a,b}

^aCollege of Information Engineering, Shanghai Maritime University, Shanghai 201306, China

^bResearch Center of Intelligent Information Processing and Quantum Intelligent Computing, Shanghai 201306, China

Abstract

Breast cancer is the second leading cause of cancer deaths among women and screening mammography has been found to reduce mortality. It is necessary to build mammography image recognition systems. Previous solutions for mammography image recognition are usually based on hand-crafted features methods and use but limited in specific situations. Also, some methods utilize simple deep learning network, which can not extract the full feature of mammography, for example, GoogleNet, VGG16, ResNet, DenseNet, etc. In this paper, we propose a deep learning based approach with multiple feature fusion transfer learning strategy. Firstly, we obtain the training data from an open data set called DDSM images. Then we employ data augment methods, and training a deep convolutional neural network to extract image features and conduct the object detection job. A pre-trained model is used to initialize the network and help extract the basic features. Furthermore, we propose a fusion method that makes use of multiple transfer learning models in inference, to improve the accuracy on the test set. Importantly, we take a strategy applied by hash learning in the deep network is cited to enhance the generalization ability of the model and solve the challenge of high-dimensional calculation in deep learning. In the end, regression analysis to analyze the object position. The experimental results prove that our method achieves high accuracy on the mammography image object detection and inspection task.

Keywords: CNNs, Random Forest, Learning to Hash, DensNet, Feature Fusion

1. Introduction

The rapid development of machine learning and especially deep learning has attracted the medical imaging community's interest in applying these techniques to improve the accuracy of cancer screening. Breast cancer is the second leading cause of cancer deaths among U.S. women and screening mammography has been proved to reduce mortality Oeffinger et al. (2015); Zhu et al. (2019). According to a study by the Breast Cancer Surveillance Consortium in 2009, the overall sensitivity of digital screening mammography in the U.S. is 84.4% and the overall specificity is

*Ri-Gui Zhou, Shihao Lv, Yaochong Li, are with the College of Information Engineering, Shanghai Maritime University, Shanghai 201306, China and the Research Center of Intelligent Information Processing and Quantum Intelligent Computing, Shanghai 201306, China.

Email addresses: rgzhou@shmtu.edu.cn (Ri-Gui Zhou), lvshihao@stu.shmtu.edu.cn (Shihao Lv), liyaochong123@gmail.com (Yaochong Li)

90.8% Jamieson et al. (2012). To help radiologists improve the predictive accuracy of screening mammography, computer-assisted detection and diagnosis (CAD) software have been developed and in clinical diagnosis since the 1990s. Unfortunately, data suggests that commercial CAD systems have not led to significant improvement in performance and progress has stagnated in the past decade Girshick (2015). With the remarkable success of deep learning in visual object recognition and detection, and many other domains have paid more attention to it Lecun et al. (2015). There is much interest in developing deep learning tools to assist radiologists and improve the accuracy of screening mammography.

Early detection of subclinical breast cancer on screening mammography is challenging as an image classification task because the tumors themselves occupy only a small portion of the image of the entire breast. For example, a full-field digital mammography (FFDM) image is typically 4000×3000 pixels while a cancerous region of interest (ROI) can be as small as 100×100 pixels. If ROI annotations were widely available in mammography databases then established object detection and classification methods such as the region-based convolutional neural network (R-CNN) and its variants could be readily applied Girshick et al. (2014); Girshick (2015); Ren et al. (2017). However, approaches that require ROI annotations Dai et al. (2016) often cannot be transferred to large mammography databases that lack ROI annotations, which are laborious and costly to assemble. Indeed, few public mammography databases are annotated. Yet, deep learning requires large training datasets to be most effective. Thus, it is essential to leverage both the few fully annotated datasets, as well as larger datasets labeled with only the cancer status of each image to improve the accuracy of breast cancer classification algorithms.

Pre-training is a promising method to address the training problem. For example Hinton et al. (2006); Li et al. (2020), used layer-wise pre-training to initialize the weight parameters of a deep belief net (DBN) with three hidden layers and then fine-tuned it for classification. They found that pre-training improved the training speed as well as the accuracy of handwritten digit recognition. Another popular training method is to first train a deep learning model on a large database such as the ImageNet Russakovsky et al. (2015); Li et al. (2020) and then fine-tune the model for another task. Although the specific task may not be related to the initial training dataset, the model’s weight parameters are already initialized for recognizing primitive features, such as edges, corners and textures, which can be readily used for a different task. This often saves training time and improves the model’s performance He et al. (2016); Moreira and Fechine (2018).

To take advantage of feature extraction ability of CNNs, recently researchers have proposed new mammography recognition methods. However, we think the ability to extract the image features of deep CNNs could be better utilized. In this study, fusing different deep neural network models together to propose a fine-grained mammography image recognition approach via fusing multiple learned features. Besides, utilizing the hash decoder method to simplifying the classification calculation of complex high-dimensional feature vectors, and fusing the results of different classifier in the end. Our work can be summarized as follows:

1. Build a deep convolutional neural network based on well-performed network structures, and design a transfer learning strategy to improve the representation power of the extracted features.
2. To further utilize the feature representation ability of CNNs, we propose a method to fuse extracted features from multiple trained models with similar topological structure to further improve the classification accuracy.
3. The strategy applied by hash learning in the deep network is cited to enhance the generalization ability of the model and solve the challenge of high-dimensional calculation in deep

learning.

4. The designed feature fusion model is used in the feature extraction process of Faster RCNN, and a deep hash learning strategy is introduced in the classification stage.

The rest of this paper is organized as follows. Section 2 details of the network structure and the proposed method. Section 3 elaborates the dataset used in our work. Section 4 demonstrates the experiment results and gives discussion. Section 5 makes the conclusion and future work are provided in the end.

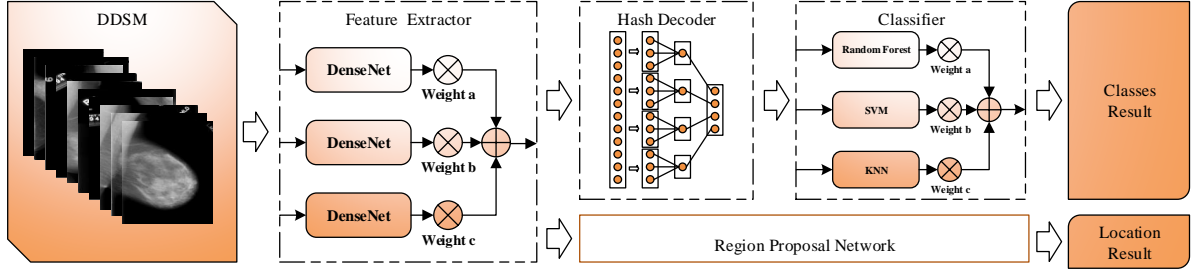


Figure 1: Overview of the proposed approach.

2. Methodology

The architecture of our approach can be divided into 4 modules, as shown in Figure 1. The first module is image feature extractor, which contains three pretrained models of DenseNet, which are trained on ImageNet task is used as the backbone of our network structure. Benefited from pre-trained models, the network gains the ability to extract basic features from images before training. Designing three different models has aimed for diverse features. To make use of different representation power of each model, fusing the feature from each model with weight add method. The second module is a hash decoder, which is aim at dividing randomly image features into multiple branches, with each branch corresponding to one hash bit. Through such steps, the model can not only improve the generalization ability of the model, but also simplify the calculation of high-dimensional features to facilitate the work of the classifier. The third module is employed to perform classification, we also has used three classifiers which contains SVM(Support Vector Machine), KNN(K Nearest Neighbor) and RF(Random Forest). This design of classifications is to help improve the accuracy of model predictions. The fourth module is a linear regression analysis model, which utilied the RPN(Region Proposal Network) proposed by Faster RCNN. To do this, it is aimed at marking the specific location of the lesion in mammography.

2.1. Network design

Hand-crafted features have been widely used in the image classification tasks, including mammography image classification tasks. Though these hand-crafted feature based methods perform well, they are always too complicated to build and could be constrained in specific situations. With the development of deep learning techniques, deep convolutional neural networks have achieved great success in image analysis task, because of its ability to extract intricate features from raw data Szegedy et al. (2016); Zeiler and Fergus (2014). By training a model with a huge amount

of images, the learned parameters network could gain greater representation power and perform better than hand-crafted feature based methods Jamieson et al. (2012). Hence we decide to build a mammography images object detection network. CNNs based approaches on mammography image recognition tasks have been proposed in recent years, most of them train a single neural network model to extract image features He et al. (2019). After AlexNet achieved great success in the ImageNet competition, the potential of deep CNNs are gradually discovered by researchers, many deep network architectures with good performance on image classification tasks such as VGGNet, GoogLeNet, ResNet, DenseNet and etc, network based on these well-performed architectures are naturally applied to mammography image recognition task. We build a fusion network made of four modules which are feature extractor(Explained in detail in Section 2.1.1), hash decoder(Explained in detail in Section 2.1.2), classifier(Explained in detail in Section 2.1.3) and regression model(Explained in detail in Section 2.1.4).

2.1.1. Feature Extract Module

In the feature extractor modules, building it with a truncated DenseNet without the fully connected layers. The backbone of DenseNet consists of 3 dense blocks, each dense block is composed of several dense layers. The number of dense layers in each dense block increases while the dense blocks go deeper. The structure of a dense block is shown in Figure 2.

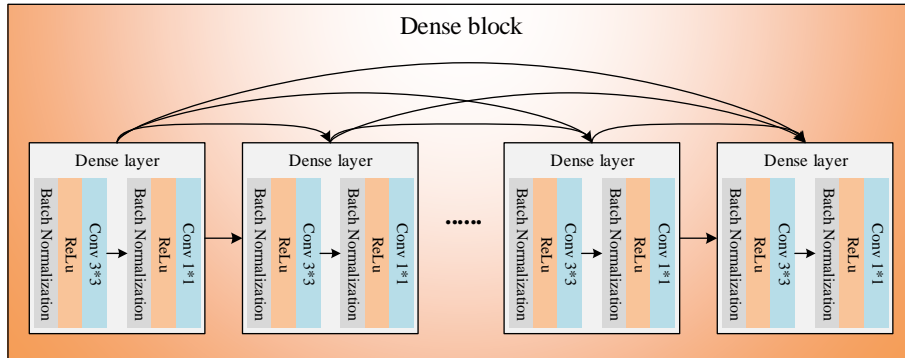


Figure 2: The architecture of DenseNet.

As for the DenseNet, different from a normal convolutional neural network, each dense layer's output is fed to all subsequent dense layers in the same block through the dense connections, which is implemented by concatenation operations. In this way, global information can traverse the dense block from beginning to end, each dense layer can acquire extra knowledge from the previous ones. For a dense layer, it includes 2 basic layers, each basic layer is composed of a batch normalization layer, a ReLU activation function Srivastava et al. (2014); Ioffe and Szegedy (2015); Kingma and Ba (2015) and 2 convolutional layers. The first convolutional layer with a 1×1 kernel is called the bottleneck layer, and it helps to reduce the feature map dimension to improve calculation efficiency. The second layer applies a 3×3 kernel to extract features. Benefit from densely connections, the network can extract more representative features than the normal convolutional network with layers connected in sequence. In addition, an attention block and a transition block are inserted between every two dense blocks. The attention block helps the feature extractors locate the most informative part of the input feature map. The transition block consists

of a batch normalization layer and a 1×1 convolutional layer followed by 2×2 max pooling layer. It is set for down sampling the output feature maps of each dense block. While network goes deeper, the size of output feature maps decreases and the dimension of output feature maps increases. An example of the output feature maps after each dense block is shown in Figure 3.

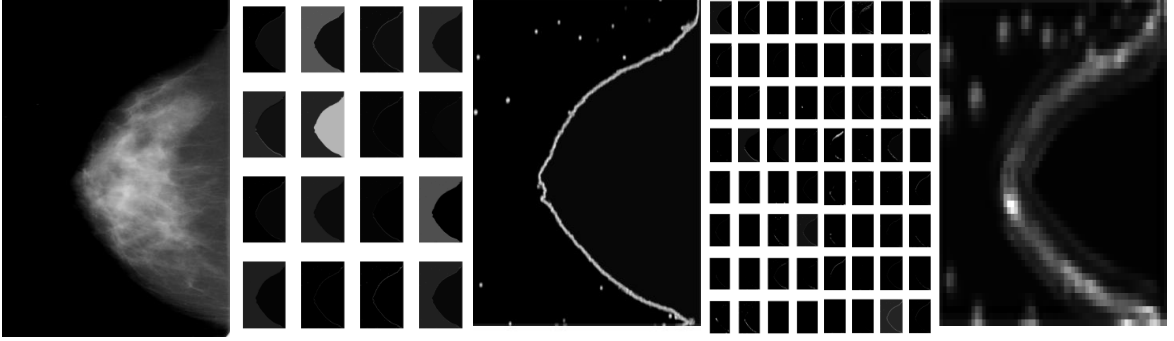


Figure 3: The feature of the fusion of extractors' result.

Usually, most CNN based methods on mammography image classification tasks use a single network to extract features, and then feed them into a classifier. However, we found that AGNet did this job in a different way. It tried to explore the potential power of fusion features extracted from different models. In which, two models are fused to predict the label of input image together, one is based on AlexNet and there is based on GoogLeNet. It takes advantage of different features with higher accuracy than the single network methods. Inspired by AGNet, proposing an approach to improve the classification accuracy by fusing multiple models with the same structure trained with different transfer learning strategies. Note that shallower layers tend to extract basic features, deeper layers tend to extract abstract feature, concluding that models with different layers' parameters fixed during the training phase would focus on features with different complexity. Ciresan et al. (2012) At the inference phase, we fuse the trained models together to make use of the different feature extraction ability of each model.

Different from AGNet, train 3 models with the same structure, but freeze different layers of each model while training concurrently. There are two reasons why we select 3 same DenseNet based model to be fused. Firstly, we have tested the single-model method for this task, among which DenseNet performs best. Secondly, we have tried fusing different trained models such as Inception, ResNet, DenseNet structures together with frozen parameters, fusing 3 DenseNet based models is still the better way. We think the reason is that when fusing models in different topological structures, the relationship between features extracted from 3 models is relatively weak and we cannot assure that they are learning different knowledge from training images. Since the structures of different networks varies greatly, models may concentrate on similar features with different performance according to the depth of network. By training 4 similar structure models with different frozen layers, each model extracts features in different levels based on the number of frozen parameters, we can ensure that every model concentrates on different features of the input image. Meanwhile, in the experiment we found the false positive and false negative instances of each model are quite different, which proves that they are concentrating on different kinds of features. Since the 4 models keep a similar network structure, the relationship between features

they extracted are stronger, and features can be fused better.

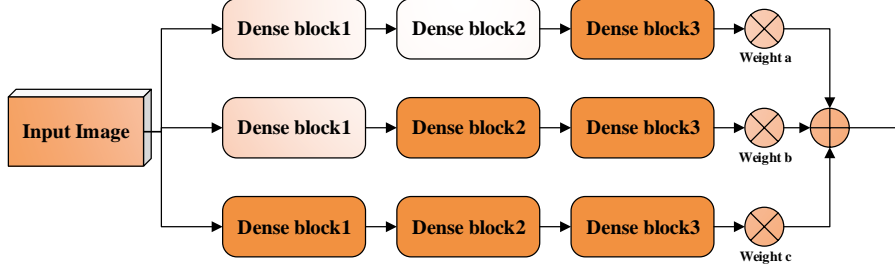


Figure 4: The module of feature extractors' fusion.

As figure 4 shows, training 3 models with parameters in different block frozen in parallel. Each row represents one model, the dense block in bright means that the parameters in this block are frozen during the training phase while the dark block means that parameters are activated. we fuse the feature of multiple transfer learning models with a weighted sum operation. The weights of 3 models are set manually in the experiments. Taking the advantage of features diversity, the transfer learning models fusion method achieved high accuracy in the mammography image recognition task.

2.1.2. Hash Decoder Module

After obtaining intermediate image features from the module of feature extractor, we propose a hash decoder module to map these image features to hash codes. We assume each target hash code has q bits. Then the outputs of the feature extractor are designed to be $50q$. As can be seen in Figure 5, the proposed hash decoder module firstly divides randomly the features vectors into q slices with equal length 4. Then each slice is mapped to one dimension by a fully-connected layer, followed by a sigmoid activation function that restricts the output value in the range $[0, 1]$, and a piece-wise threshold function to encourage the output of binary hash bits. After that, the q output hash bits are concatenated to be a q -bit code. A possible alternative to the hash decoder module is a simple fully-connected layer that maps the input intermediate image features into q -dimensional vectors, followed by sigmoid activation functions to transform these vectors into $[0, 1]$. Compared to this alternative, the key idea of the overall strategy is trying to reduce the redundancy among the hash bits. Hash codes with fewer redundant bits are advocated by some recent research.

In order to encourage the output of a hash decoder to be binary codes, we use a sigmoid activation function followed by a piece-wise threshold function. Given a 50-dimensional slice $x^{(i)} (i = 1, 2, \dots, q)$, the output of the 50-to-1 fully-connected layer is defined by

$$fc_i(x^{(i)}) = W_i x^{(i)} \quad (1)$$

with W_i being the weight matrix.

Given $c = fc_i(x^{(i)})$, the sigmoid function is defined by

$$\text{sigmoid}(c) = \frac{1}{1 + e^{-\beta c}} \quad (2)$$

where β is a hyper-parameter.

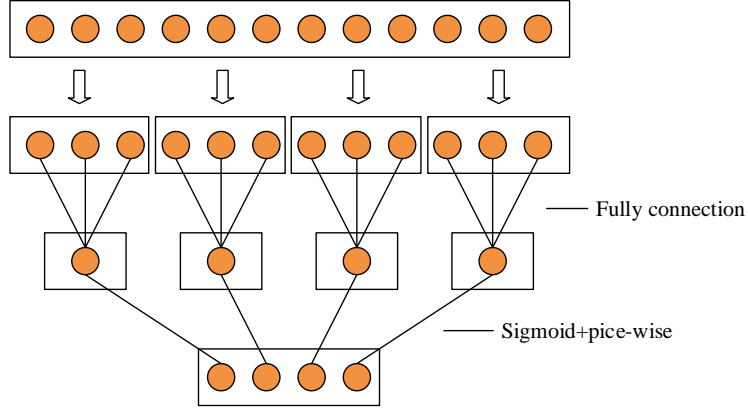


Figure 5: The module of the hash decoder.

The piece-wise threshold function is to encourage binary outputs. Specifically, for an input variable $s = \text{sigmoid}(c) \in [0, 1]$, this piece-wise function is defined by

$$y = \begin{cases} 0, & s < 0.5 - \epsilon \\ s, & 0.5 - \epsilon \leq s \leq 0.5 + \epsilon \\ 1, & s > 0.5 + \epsilon \end{cases},$$

where ϵ is a small positive hyper-parameter.

This piece-wise threshold function approximates the behavior of hard-coding, and it encourages binary outputs in training. Specifically, if the outputs from the sigmoid function are in $[0, 0.5 - \epsilon]$ or $[0.5 + \epsilon, 1]$, they are truncated to be 0 or 1, respectively. Note that in prediction, the proposed deep architecture only generates approximate (real-value) hash codes for input images, where these approximate codes are converted to binary codes by quantization. With the proposed piece-wise threshold function, some of the values in the approximate hash codes are already zeros or ones. Hence, less errors may be introduced by the quantization step.

2.1.3. Classifier Module

In the classifier module, building it with a fusion structure by SVM, KNN, Random Forest classic methods. For each method, it predicates with the output of the hash decoder, then the three results weight add, as the result of class information. There is a reason why we select 3 different classifiers to be fused. These three algorithms target different classification types, so the results obtained for different feature information will also be different. The biggest advantage of doing this is to improve the robustness of the model, and at the same time it also improves the accuracy of model recognition.

As for the KNN, which is simple, easy to understand, easy to implement, no need to estimate parameters, no training. As for the SVM, after the training is completed, most of the training samples do not need to be retained, and the final model is only related to the support vector. As for the Random Forest, which is based on an ensemble of decision trees where each of the trees is based on the randomly selected subset of the training set. Random forest uses slightly different kinds of bagging approach where a subset of features is selected for the split at node, whereas in

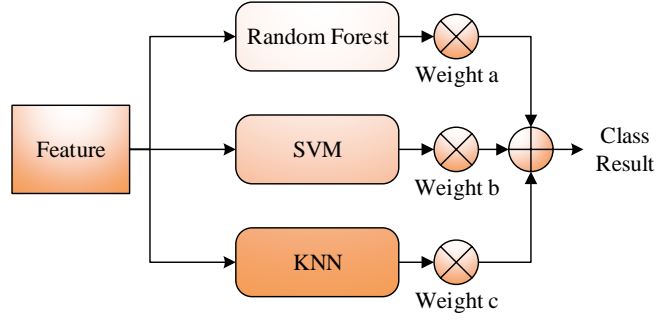


Figure 6: The module of the fusion of classifier.

bagging all features are used for node split. As a result, the random forest is an aggregation of trees, which reduces the effect of noise present in a single tree. Hence, bagging generally increases the overall result.

2.1.4. Regression module

A Region Proposal Network (RPN) takes an image (of any size) as input and outputs a set of rectangular object proposals, each with an objectness score. To generate region proposals, sliding a small network over the conv feature map output by the last shared conv layer. This network is fully connected to an $n \times n$ spatial window of the input conv feature map. Each sliding window is mapped to a lower-dimensional vector. This vector is fed into two sibling fully-connected layers — a box-regression layer and a box-classification layer. As shown in Figure 7

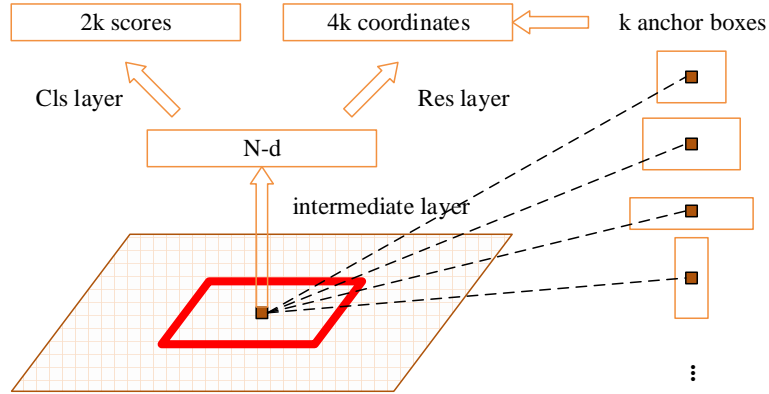


Figure 7: The module of the region proposal network.

Note that because the mini-network operates in a sliding-window fashion, the fully-connected layers are shared across all spatial locations. This architecture is naturally implemented with an $n \times n$ conv layer followed by two sibling 1×1 conv layers. And the loss function is defined by

$$L(p_i, t_i) = \frac{1}{N_{cls}} \sum_i L_{cls}(p_i, p_i^*) + \lambda \frac{1}{N_{reg}} \sum_i p_i^* L_{reg}(t_i, t_i^*) \quad (3)$$

Here, i is the index of an anchor in a mini-batch and p_i is the predicted probability of anchor i being an object. The ground-truth label p_i^* is 1 if the anchor is positive, and is 0 if the anchor is negative. t_i is a vector representing the 4 parameterized coordinates of the predicted bounding box, and t_i^* is that of the ground-truth box associated with a positive anchor. The classification loss L_{cls} is log loss over two classes (object *vs* not object). For the regression loss, we use $L_{reg}(t_i, t_i^*) = R(t_i, t_i^*)$ where R is the robust loss function (smooth L_i). The term $p_i^* L_{reg}$ means the regression loss is activated only for positive anchors and is disabled otherwise. The outputs of the *cls* and *reg* layers consist of p_i and t_i respectively. The two terms are normalized with N_{cls} and N_{reg} , and a balancing weight λ .

For regression, we adopt the parameterizations of the 4 coordinates following:

$$t_x = (x - x_a)/w_a, t_y = (y - y_a)/h_a, t_w = \log(w/w_a), t_h = \log(h/h_a), \quad (4)$$

$$t_x^* = (x^* - x_a^*)/w_a, t_y^* = (y^* - y_a^*)/h_a, t_w^* = \log(w^*/w_a), t_h^* = \log(h^*/h_a) \quad (5)$$

where x , y , w , and h denote the two coordinates of the box center, width, and height. Variables x , x_a , and x^* are for the predicted box, anchor box, and ground-truth box respectively (likewise for y , w , h). This can be thought of as bounding-box regression from an anchor box to a nearby ground-truth box.

2.2. Transfer learning

Transfer learning aims to transfer knowledge between related source and target domains Pan and Yang (2010). It is a useful tool in machine learning, leading to a positive effect on the domains that are difficult to apply because of insufficient training data. Transfer learning methods can be categorized into 4 classes: instance-based, mapping-based, network-based, adversarial-based deep transfer learning Tan et al. (2018). Network-based method is mostly used in convolutional neural networks. It is achieved by transferring the network structure and pre-trained parameters of the source domain into a part of a deep convolutional neural network used in the target domain. In our work, we construct feature extractor as described in Section 2.1.1, then we initialize the network parameters with the parameters of a DenseNet model that were pre-trained on the ImageNet dataset.

In our experiments, an input image is resized to a tensor, going that dataset; freezing, which consists of leaving the parameters in shallow part of the pretrained model unchanged and training only the rest part of the network, which can make use of the basic feature extracting ability of pretrained model. Freezing layers or not in training phase depends on the number of category and quantity variance between source and target dataset. Compared to ImageNet dataset, the DDSM dataset we used are much smaller. Moreover, most images in both datasets are natural images, they are similar in a way, hence we freeze some of the layers during training. In order to explore the effect of fusing different feature extractors, we try different freezing strategy on the networks, the details are described in Section 2.1.1.

3. Data

3.1. DDSM

Most computer-aided diagnosis (CADx) and detection (CAdE) algorithms for breast cancer in mammography are evaluated on private data sets or on unspecified subsets of public databases. Gao et al. (2019) This causes an inability to directly compare the performance of methods or to replicate prior results. Choukroun et al. (2017) To resolve this substantial challenge by releasing an updated and standardized version of the Digital Database for Screening Mammography (DDSM) for evaluation of future CADx and CAdE systems (sometimes referred to generally as CAD) research in mammography. Zhu et al. (2017) The CBIS-DDSM (Curated Breast Imaging Subset of DDSM), includes decompressed images, data selection, curation by trained mammographers, updated mass segmentation, bounding boxes, and pathologic diagnosis for training data, formatted similarly to modern computer vision data sets. The data set contains 753 calcification cases and 891 mass cases, providing a data-set size capable of analyzing decision support systems in mammography. As shown in Figure 8

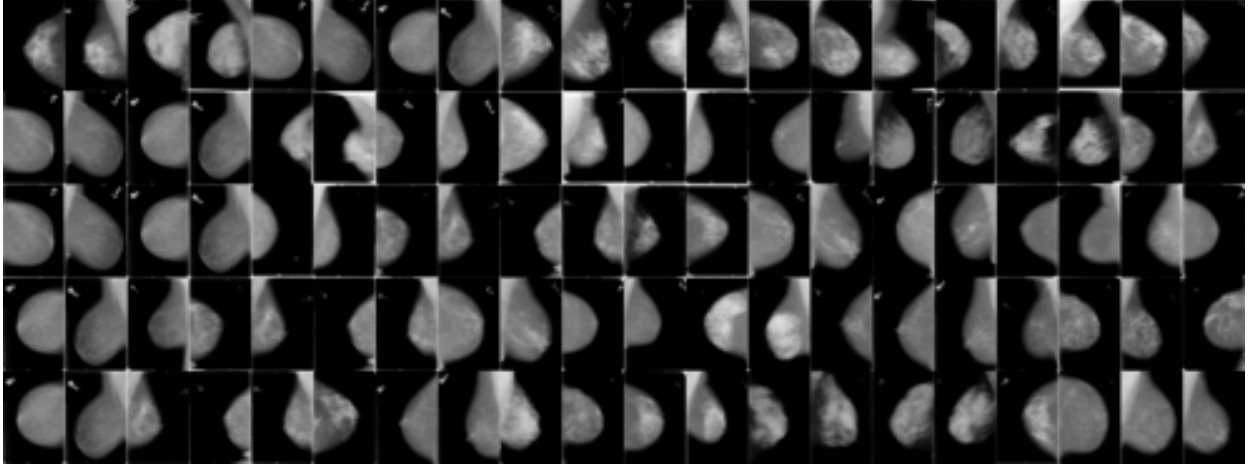


Figure 8: Examples in the dataset

3.2. Augmentation

Compared to other common data sets (e.g. Pascal Voc) in the field of image object detection, the DDSM data set is relatively small. M. Heath, K. Bowyer, D. Kopans and Jr. (2001) Since small data sets are prone to reduce the model effect, to maintain the representation power of model and avoid overfitting in some ways, several data augmentation methods are employed. We don't augment data with the crop, translate or scale operations to avoid changing the original label of images. Instead, we randomly rotate and shear the original images between -10° and 10° , then flip them horizontally or vertically and fill the margin with white pixels.

4. Experiments

4.1. Training strategies

The approach of this study is implemented by the open source framework PyTorch. Abadi et al. (2016) The pre-trained models for initializing the network parameters are acquired from

torchvision. Paszke et al. (2017) Models are trained and tested on a graphic workstation with an Intel Core i9-7980XE CPU(2.60 GHz, 18 core) and a GeForce GTX 1080Ti GPU. As described in Section 3, we choose a dataset DDSM to train and test our proposed network in the experiments.

In the training phase, we use a stochastic gradient descent method with a batch size of 32, Ioffe and Szegedy (2015) a momentum of 0.9 and a weight decay of 0.0005 similar to optimize our models for 100 epochs. As shown in Figure 4, we propose a method fusing 3 models with similar structure and freezing different layers called Freeze1 to Freeze3 from top to bottom. The accuracy curves on the validation dataset of 3 models in the training phase are shown in Figure 9. Due to the warmup strategy, Glorot et al. (2011) the accuracy grows slowly in the first 5 epochs. A relatively large batch size reduces the noise in the gradient, and an increased learning rate can make a larger progress along the opposite of the gradient direction. Liu and Lapata (2020) Since our network structure is based on DenseNet, the learning rate is initialized to 0.01 and lowered by 10 times every 20 epochs in the experiments. Jia et al. (2014)

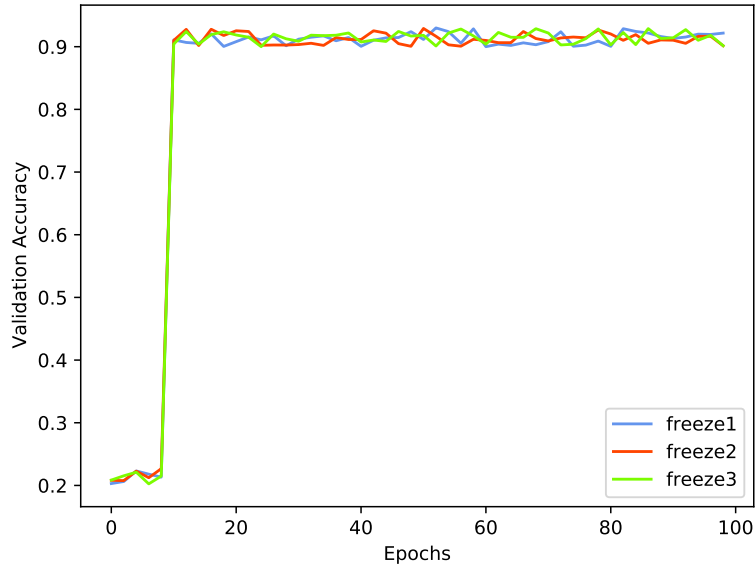


Figure 9: Validation accuracy.

Although the parameters of the network were initialized with the model trained by ImageNet at the beginning of the training phase, and the model is far from the final solution, we adopt a warmup strategy by using a very small learning rate 0.00001 in the first 5 epochs and then switch to the initial learning rate when the training process is stable. Besides, for every 5 epochs, we compare the performance between the current model and the best model of previous epochs. If the previous one performs better, the parameters in the former model will be loaded into the current model before the next epoch starts.

4.2. Results

For mammography image recognition, the DDSM dataset contains 753 calcification cases, providing a data-set size capable of analyzing decision support systems in mammography. We also compared the results on the DDSM dataset with other methods including CNN feature-based methods. As shown in Table 1, the proposed method achieved high accuracy close to other methods without obvious advantages on the DDSM dataset. We also trained 3 models concentrating

on different kind of features by freezing different parameters during training. This method performs better on a fine-grained classification task. Our method achieved high accuracy on this task, significantly higher than other methods.

Table 1: Performance comparing to different methods

Method	Accuracy(%)
SIFT-BoVW	89.05
VGGNet	90.01
AGNet	91.28
Inception	93.48
DenseNet	93.70
Our	94.68

4.3. Statistical analysis of fusion method

In the previous sections, we have proposed a method which fuses 3 models with different layers' parameters frozen to improve performance, particularly in Section 2.1.1 we mention that different models concentrate on different aspects of input images. To evaluate the diversity of 3 models, we conduct statistical analysis with a series of ablation studies.

Firstly, we try to fuse any 2 models of 3 models with different frozen parameters and calculate their accuracies on the test set comparing to a single model. Details of the results are listed in Table 2. F1-F4 represent model Freeze1 to Freeze4 respectively and & means fusing two models together, for instance, F1&F2 means fusing model Freeze1 and Freeze2. According to the results, we find that fusing any of 2 models always performs better than a single one for each category. It can be concluded that models with different layers' parameters frozen focus on different features of images in different categories, which leads to the fused network model get better performance.

Table 2: Results of fusing any 2 models

Category	F1(%)	F2(%)	F3(%)	F1&F2(%)	F1&F3(%)	F2&F3(%)
1	90.55	89.60	92.06	92.30	93.05	93.05
2	89.03	91.13	93.37	92.08	96.02	97.06
3	90.37	93.02	91.07	93.51	93.60	94.05
4	88.70	88.67	89.06	92.07	93.05	94.08
5	89.50	89.60	90.05	92.30	94.70	95.05
6	92.06	89.09	94.06	91.03	94.03	97.04
7	91.05	89.60	92.06	92.30	93.05	96.02

In addition, when testing each single network's performance, we count the numbers of instances that only one model recognizes them wrongly while the other three predict correctly. As shown in columns from 3 to 6 in Table 3, 3 models don't give the same predicting result of every image in each category. For each category, there are dozens of images which recognized wrongly by only one model, and the other 2 models can recognize them better.

And It can be observed that none of the images are wrongly recognized by all the 3 models at the same time, from the last column in Table 3. In other words, the 3 models pay attention to different

Table 3: Comparison of number of images recognized wrongly by only one model

Category	Total	Freeze1	Freeze2	Freeze3	All
1	1172	58	44	31	0
2	1029	24	29	36	0
3	1105	36	61	44	0
4	859	48	41	56	0
5	786	76	87	36	0
6	907	15	29	41	0
7	937	80	29	64	0

aspects of the images, and each model has its advantage and drawback. By integrating them and fusing their extracted diversified features together, the ensemble model learns more representative features.

4.4. Analysis the hash decoder

In this work, one of the innovation points, is to employ a hash decoder to reduce the difficulty of computing the high dimension parameters. A natural alternative to the hash decoder is a simple fully-connected layer followed by a sigmoid layer of restricting the output values' range in $[0, 1]$. To investigate the effectiveness of the hash decoder. Implement and evaluate a single deep network-based DenseNet, connecting with its alternative choice which is a fully network. In the end, we employ a single classifier based SVM. To do this, to prove our hash decoder is effective. As can be seen from Table 4, the results of the proposed method outperform the competitor with the alternative. For example, the architecture with hash decoder achieves the accuracy of 0.581 with 48 bits, which indicates an improvement of 19.7% over the FC alternative. The underlying reason for the improvement may be that, compared to the FC alternative, the output hash codes from the hash decoder are less redundant to each other.

Table 4: Comparison results of the hash decoder and fully connection

Method(MAP)	12 bits	24 bits	32 bits	48 bits
FC	0.877	0.896	0.909	0.912
Ours	0.899	0.914	0.925	0.923

4.5. Comparing to the single classifier

To investigate the effectiveness of the fusion of the classifiers. A single DenseNet is employed for this experiment, because it can maintain the invariance of the feature vector and enlarging the impact of classifier differences on test results. The specific experimental results are shown in the Table 5. From the data in the table, we can see that the difference between different classifiers is more obvious, and the effect of random forest is better, but the result of the fused classifier is the best. The reason for this is that the principle of different classifiers is different and the sensitivity of features is different. It is obvious that the results of the fusion classifier can make the accuracy more reliable.

Table 5: Comparison results of the classifiers

Classifier	Accuracy(%)
k-NN	83.50
SVM	85.70
RandomForest	87.09
Ours	91.49

4.6. Comparing to single network methods

There have been approaches with single network structures applied on DDSM, well-performed structures like VGGNet, Inception, ResNet and etc are used as the backbones for constructing the networks of mammography image recognition approaches. To figure out which backbone is most suitable for this task, the experiments are conducted to test the performance of the network with different backbones. Figure 10 shows the accuracy of several backbones we tried on the validation set during 100 training epochs. In the first 5 epochs, the accuracy grows slowly because of the warmup strategy mentioned in Section 4.1, and the learning rate is set to a relatively small value before the training process is stable. We found the accuracy of DenseNet is slightly higher than other models in the experiment. Hence it is used as one of the backbones.

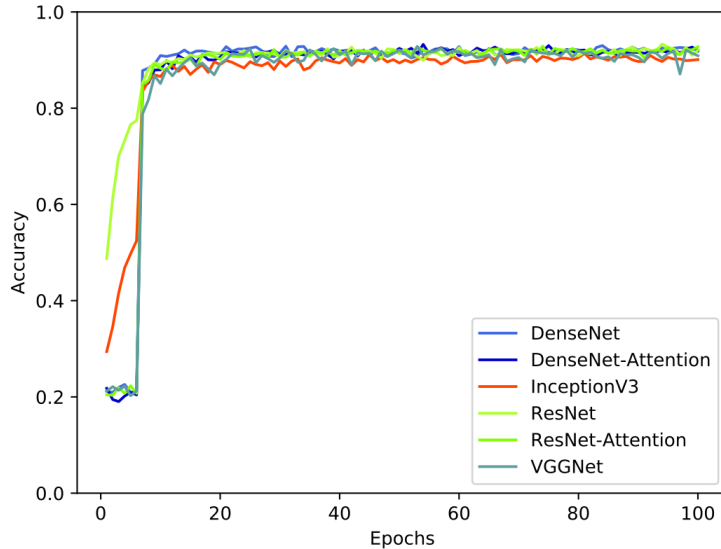


Figure 10: Validation accuracy of different backbone.

The proposed transfer learning model fusion method is shown in Figure 4, 3 models are trained in parallel with different frozen parameters. weight of each model is set manually according to the singles model's accuracy. The accuracy of each single model with different frozen parameters is shown in Table 7. For instance, model Freezel represents the top row in Figure 4, which is the model with the most frozen parameters. In our work, we test different weights for each model according to their accuracies on the validation set, as shown in Figure 9. Lastly, the weights for 3 models are set to $[0.4, 0.4, 0.3]$.

4.7. Comparing different network fusion methods

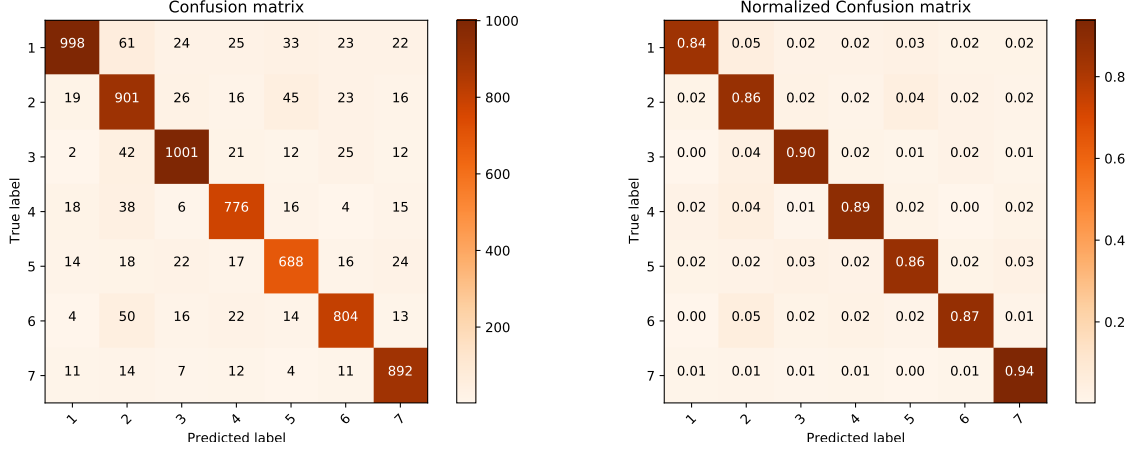


Figure 11: Confusion matrices produced by the first frozen models on the test set

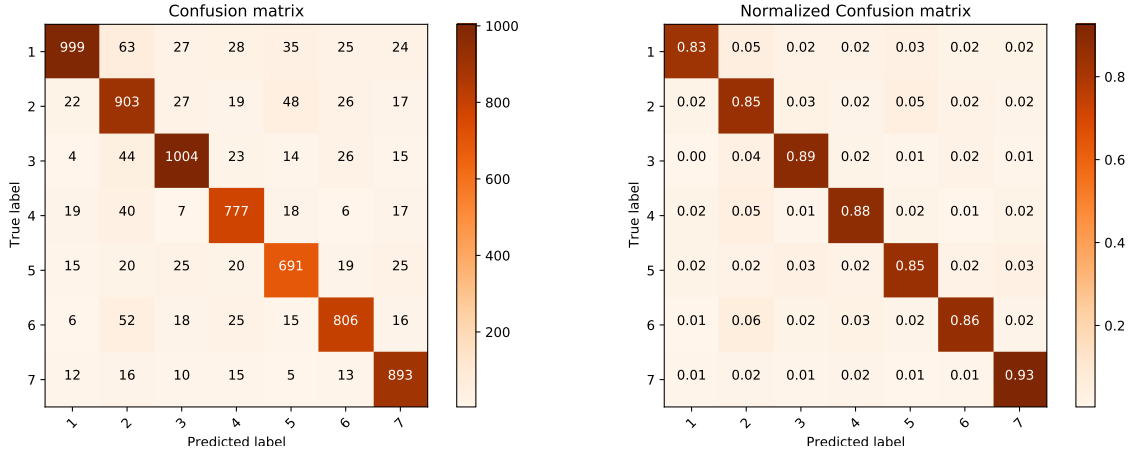


Figure 12: Confusion matrices produced by the second frozen models on the test set

Table 6: Comparing with the single network based methods on DDSM dataset

Method	Accuracy(%)	Average inference time (ms)
VGGNet based	90.09	6.062
InceptionV3 based	92.16	2.396
ResNet50 based	93.08	3.006
DenseNet based	92.67	3.762
Our	94.48	15.052

We have proposed a method of fusing 3 models with different network structure but different frozen parameters. This idea is inspired by AGNet, a method enriching extracted features by combining 2 networks with a weighted sum. Due to the different topological structures, the relationship

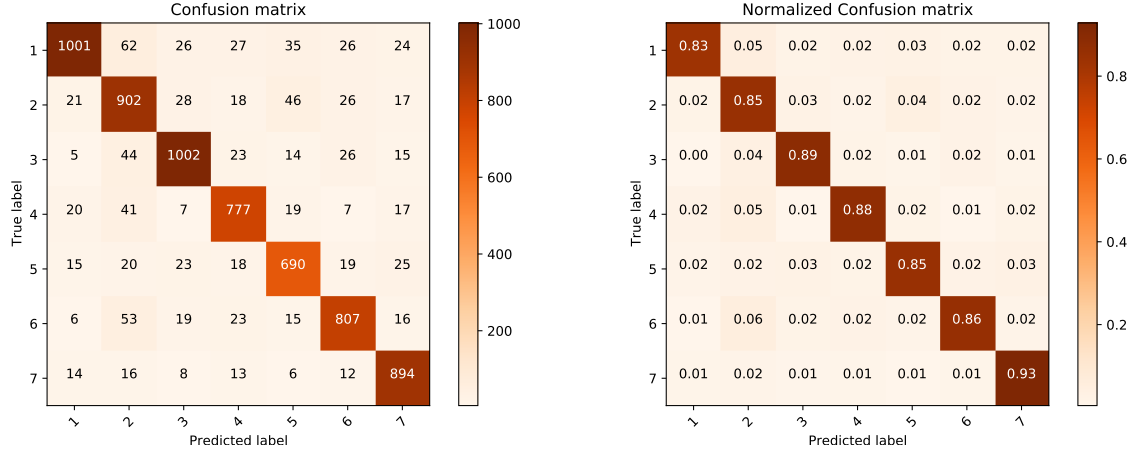


Figure 13: Confusion matrices produced by the thirty frozen models on the test set

between features they extracted is relatively weak and we cannot assure that they have learned knowledge of different aspects from the training images.

Table 7: Accuracies of models with different parameters frozen

Models	Freeze params	Test accuracy(%)
Freeze1	4.76M	93.01
Freeze2	3.50M	92.36
Freeze3	0.95M	91.88
Fusion	-	94.48

In the experiments, we test the methods of fusing models in different network structures and on the DDSM dataset. As shown in Figure 11 to Figure 13, among the 3 models we trained, Freeze3 achieves the best result on the validation set during the training phase. Therefore, we try to fuse it with other models in different network structure such as VGGNet, Inception, ResNet to check whether the fusion models in different network structure helps improve the performance or not. The parameters of these models are initialized by the corresponding pre-trained model on ImageNet and their shallow layers are frozen while training. According to the results listed in Table 6, compared to the single network-based method, it has higher accuracy, but fusing 3 models still performs better. In this way, the network extracts more rich features and the classifier produces better recognition results.

Figure 14 shows the classification results of each class with confusion matrix. The accuracies of 7 classes are higher than 92%. Because the features are learned from the training set and there are some overlapping image parts between classes, which contain a large images are more likely be wrongly classified.

4.8. Comparing other object detection methods

For the target detection module of this work, it is mainly based on the Faster RCNN framework, and the innovation of this study is also the innovation of the classification stage. For the object detection module, we made a simple comparison with the original framework model in terms of

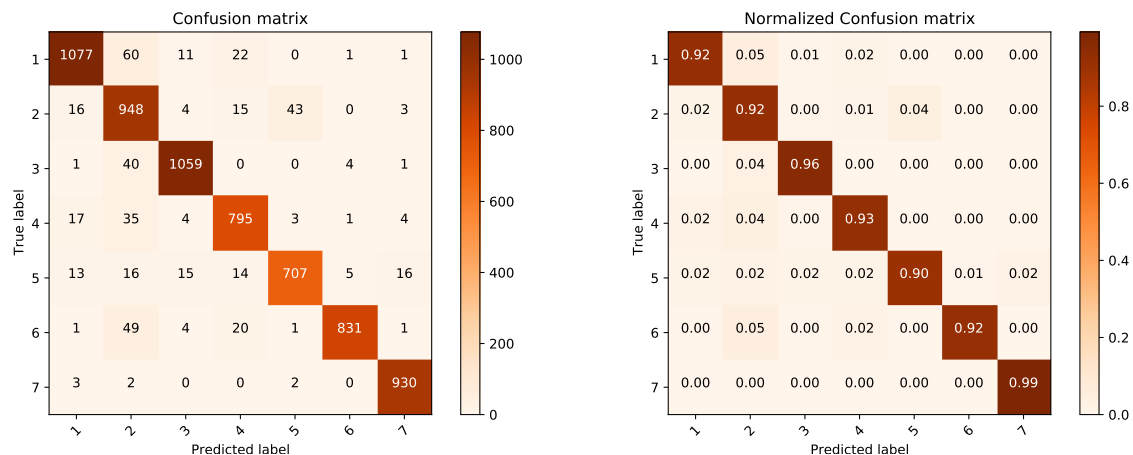


Figure 14: Confusion matrices produced by the fusion model on the test set.

time and accuracy. The specific experimental results are shown in Table 8. It is obvious from the data in the table that our method greatly improves the calculation time of the model without losing accuracy. Combining with our model framework, the reason can be clearly found because we have introduced a hash recoder module.

Table 8: Comparing to the region RCNN

Models	mAP(%)	time(ms)
Fast RCNN	60.50	534
Faster RCNN	70.03	325
Ours	75.01	105

5. Conclusion

In this paper, a deep convolutional neural network for mammography images object detection task, which employing the strategy of combining multiple model fusion transfer and transfer learning to improve the classification accuracy. Taking advantage of multiple models' representation power, the proposal achieves a higher accuracy than merely a single model. Meanwhile, the strategy applied by hash learning in the deep network is cited to enhance the generalization ability of the model and solve the challenge of high-dimensional calculation in deep learning. In the experiments, it's found that classifying images based on CNN relies heavily on the quantity and breadth of the training data set. Our network is still not efficient enough to cover every situation of mammography diagnosed. In the future, we plan to collect a larger data set with more detailed labels and build a more effective architecture to further improve the performance of the mammography image object detection.

6. Acknowledgements

This work is supported by the National Key R&D Plan under Grant No. 2018YFC1200200 and 2018YFC1200205; Shanghai Science and Technology Project in 2020 under Grant No. 20040501500.

References

- Abadi, M., Barham, P., Chen, J., Chen, Z., Davis, A., Dean, J., Devin, M., Ghemawat, S., Irving, G., Isard, M., Kudlur, M., Levenberg, J., Monga, R., Moore, S., Murray, D. G., Steiner, B., Tucker, P., Vasudevan, V., Warden, P., Wicke, M., Yu, Y., Zheng, X., 2016. TensorFlow: A system for large-scale machine learning. In: Proceedings of the 12th USENIX Symposium on Operating Systems Design and Implementation, OSDI 2016.
- Choukroun, Y., Bakalo, R., Ben-Ari, R., Askelrod-Ballin, A., Barkan, E., Kisilev, P., 2017. Mammogram classification and abnormality detection from nonlocal labels using deep multiple instance neural network. In: VCBM 2017 - Eurographics Workshop on Visual Computing for Biology and Medicine.
- Çiğreşan, D. C., Giusti, A., Gambardella, L. M., Schmidhuber, J., 2012. Deep neural networks segment neuronal membranes in electron microscopy images. In: Advances in Neural Information Processing Systems.
- Dai, J., Li, Y., He, K., Sun, J., 2016. R-FCN: Object detection via region-based fully convolutional networks. In: Advances in Neural Information Processing Systems.
- Gao, X., Braden, B., Taylor, S., Pang, W., 2019. Towards real-time detection of squamous pre-cancers from oesophageal endoscopic videos. In: Proceedings - 18th IEEE International Conference on Machine Learning and Applications, ICMLA 2019.
- Girshick, R., 2015. Fast R-CNN. In: Proceedings of the IEEE International Conference on Computer Vision.
- Girshick, R., Donahue, J., Darrell, T., Malik, J., 2014. Rich feature hierarchies for accurate object detection and semantic segmentation. In: Proceedings of the IEEE Computer Society Conference on Computer Vision and Pattern Recognition.
- Glorot, X., Bordes, A., Bengio, Y., 2011. Deep sparse rectifier neural networks. In: Journal of Machine Learning Research.
- He, K., Zhang, X., Ren, S., Sun, J., 2016. Deep residual learning for image recognition. In: Proceedings of the IEEE Computer Society Conference on Computer Vision and Pattern Recognition.
- He, T., Zhang, Z., Zhang, H., Zhang, Z., Xie, J., Li, M., 2019. Bag of tricks for image classification with convolutional neural networks. In: Proceedings of the IEEE Computer Society Conference on Computer Vision and Pattern Recognition.
- Hinton, G. E., Osindero, S., Teh, Y. W., 2006. A fast learning algorithm for deep belief nets. Neural Computation.
- Ioffe, S., Szegedy, C., 2015. Batch normalization: Accelerating deep network training by reducing internal covariate shift. In: 32nd International Conference on Machine Learning, ICML 2015.
- Jamieson, A. R., Drukker, K., Giger, M. L., 2012. Breast image feature learning with adaptive deconvolutional networks. In: Medical Imaging 2012: Computer-Aided Diagnosis.
- Jia, Y., Shelhamer, E., Donahue, J., Karayev, S., Long, J., Girshick, R., Guadarrama, S., Darrell, T., 2014. Caffe: Convolutional architecture for fast feature embedding. In: MM 2014 - Proceedings of the 2014 ACM Conference on Multimedia.
- Kingma, D. P., Ba, J. L., 2015. Adam: A method for stochastic optimization. In: 3rd International Conference on Learning Representations, ICLR 2015 - Conference Track Proceedings.
- Lecun, Y., Bengio, Y., Hinton, G., 2015. Deep learning.
- Li, Y., Zhou, R., Xu, R., Luo, J., Jiang, S., 2020. A quantum mechanics-based framework for eeg signal feature extraction and classification. IEEE Transactions on Emerging Topics in Computing, 1-1.
- Li, Y., Zhou, R.-G., Xu, R., Luo, J., Hu, W., 2020. A quantum deep convolutional neural network for image recognition. Quantum Science and Technology 5 (4), 44003.
URL <https://doi.org/10.1088/2202-2058-9565/2/2Fab9f93>
- Liu, Y., Lapata, M., 2020. Text summarization with pretrained encoders. In: EMNLP-IJCNLP 2019 - 2019 Conference on Empirical Methods in Natural Language Processing and 9th International Joint Conference on Natural Language Processing, Proceedings of the Conference.
- M. Heath, K. Bowyer, D. Kopans, R. M., Jr., P. K., 2001. The Digital Database for Screening Mammography. In: the Fifth International Workshop on Digital Mammography, M.J. Yaffe, ed., Medical Physics Publishing, 2001.
- Moreira, D. C., Fachine, J. M., 2018. A Machine Learning-based Forensic Discriminator of Pornographic and Bikini Images. In: Proceedings of the International Joint Conference on Neural Networks.
- Oeffinger, K. C., Fontham, E. T., Etzioni, R., Herzig, A., Michaelson, J. S., Shih, Y. C. T., Walter, L. C., Church, T. R., Flowers, C. R., LaMonte, S. J., Wolf, A. M., DeSantis, C., Lortet-Tieulent, J., Andrews, K., Manassaram-Baptiste, D., Saslow, D., Smith, R. A., Brawley, O. W., Wender, R., 2015. Breast cancer screening for women at average risk: 2015 Guideline update from the American cancer society.

- Pan, S. J., Yang, Q., 2010. A survey on transfer learning.
- Paszke, A., Gross, S., Chintala, S., Chanan, G., Yang, E., Facebook, Z. D., Research, A. I., Lin, Z., Desmaison, A., Antiga, L., Srl, O., Lerer, A., 2017. Automatic differentiation in PyTorch. In: Advances in Neural Information Processing Systems.
- Ren, S., He, K., Girshick, R., Sun, J., 2017. Faster R-CNN: Towards Real-Time Object Detection with Region Proposal Networks. IEEE Transactions on Pattern Analysis and Machine Intelligence.
- Russakovsky, O., Deng, J., Su, H., Krause, J., Satheesh, S., Ma, S., Huang, Z., Karpathy, A., Khosla, A., Bernstein, M., Berg, A. C., Fei-Fei, L., 2015. ImageNet Large Scale Visual Recognition Challenge. International Journal of Computer Vision.
- Srivastava, N., Hinton, G., Krizhevsky, A., Sutskever, I., Salakhutdinov, R., 2014. Dropout: A simple way to prevent neural networks from overfitting. Journal of Machine Learning Research.
- Szegedy, C., Vanhoucke, V., Ioffe, S., Shlens, J., Wojna, Z., 2016. Rethinking the Inception Architecture for Computer Vision. In: Proceedings of the IEEE Computer Society Conference on Computer Vision and Pattern Recognition.
- Tan, C., Sun, F., Kong, T., Zhang, W., Yang, C., Liu, C., 2018. A survey on deep transfer learning. In: Lecture Notes in Computer Science (including subseries Lecture Notes in Artificial Intelligence and Lecture Notes in Bioinformatics).
- Zeiler, M. D., Fergus, R., 2014. Visualizing and understanding convolutional networks. In: Lecture Notes in Computer Science (including subseries Lecture Notes in Artificial Intelligence and Lecture Notes in Bioinformatics).
- Zhu, W., Lou, Q., Vang, Y. S., Xie, X., 2017. Deep multi-instance networks with sparse label assignment for whole mammogram classification. In: Lecture Notes in Computer Science (including subseries Lecture Notes in Artificial Intelligence and Lecture Notes in Bioinformatics).
- Zhu, Z., Albadawy, E., Saha, A., Zhang, J., Harowicz, M. R., Mazurowski, M. A., 2019. Deep learning for identifying radiogenomic associations in breast cancer. Computers in Biology and Medicine.